

UNCLASSIFIED

NAVAL AIR WARFARE CENTER AIRCRAFT DIVISION
PATUXENT RIVER, MARYLAND



TECHNICAL MEMORANDUM

REPORT NO: NAWCADPAX/TM-2000/91

MECHANICAL PROPERTIES OF 7076-T6 ALUMINUM ALLOY

by

Kenneth George
Eun U. Lee
Philip M. Reineke

3 August 2000

20000920 073

Approved for public release; distribution is unlimited.

UNCLASSIFIED

DEPARTMENT OF THE NAVY
NAVAL AIR WARFARE CENTER AIRCRAFT DIVISION
PATUXENT RIVER, MARYLAND

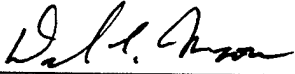
NAWCADPAX/TM-2000/91
3 August 2000

MECHANICAL PROPERTIES OF 7076-T6 ALUMINUM ALLOY

by

Kenneth George
Eun U. Lee
Philip M. Reineke

RELEASED BY:

 8/3/00

DALE MOORE / DATE
Director, Materials Competency
Naval Air Warfare Center Aircraft Division

REPORT DOCUMENTATION PAGE				Form Approved OMB No. 0704-0188	
Public reporting burden for this collection of information is estimated to average 1 hour per response, including the time for reviewing instructions, searching existing data sources, gathering and maintaining the data needed, and completing and reviewing this collection of information. Send comments regarding this burden estimate or any other aspect of this collection of information, including suggestions for reducing this burden, to Department of Defense, Washington Headquarters Services, Directorate for Information Operations and Reports (0704-0188), 1215 Jefferson Davis Highway, Suite 1204, Arlington, VA 22202-4302. Respondents should be aware that notwithstanding any other provision of law, no person shall be subject to any penalty for failing to comply with a collection of information if it does not display a currently valid OMB control number. PLEASE DO NOT RETURN YOUR FORM TO THE ABOVE ADDRESS.					
1. REPORT DATE 3 August 2000		2. REPORT TYPE Technical Memorandum		3. DATES COVERED January - November 1999	
4. TITLE AND SUBTITLE Mechanical Properties of 7076-T6 Aluminum Alloy				5a. CONTRACT NUMBER	
				5b. GRANT NUMBER	
				5c. PROGRAM ELEMENT NUMBER	
6. AUTHOR(S) Kenneth George Eun U. Lee Philip M. Reineke				5d. PROJECT NUMBER	
				5e. TASK NUMBER	
				5f. WORK UNIT NUMBER	
7. PERFORMING ORGANIZATION NAME(S) AND ADDRESS(ES) Naval Air Warfare Center Aircraft Division 22347 Cedar Point Road, Unit #6 Patuxent River, Maryland 20670-1161				8. PERFORMING ORGANIZATION REPORT NUMBER NAWCADPAX/TM-2000/91	
9. SPONSORING/MONITORING AGENCY NAME(S) AND ADDRESS(ES) Naval Air Systems Command 47123 Buse Road Unit IPT Patuxent River, Maryland 20670-1547				10. SPONSOR/MONITOR'S ACRONYM(S)	
				11. SPONSOR/MONITOR'S REPORT NUMBER(S)	
12. DISTRIBUTION/AVAILABILITY STATEMENT Approved for public release; distribution is unlimited.					
13. SUPPLEMENTARY NOTES					
14. ABSTRACT This report documents a collaborative material characterization study of 7076-T6 forged aluminum performed by the NAVAIRSYSCOM Materials Division and Hamilton Sundstrand, sponsored and coordinated by the NAVAIRSYSCOM Engineering Specialties Division. The purpose was to determine the mechanical properties of the alloy to support the development of a fatigue allowables curve used for life assessment of 54H60 propeller blades. Specimens were fabricated from unused propeller forgings and tested at room temperature in ambient laboratory conditions using servo-hydraulic mechanical testing equipment. Tensile properties, fatigue crack growth rates, and stress life behavior were characterized using standard ASTM test procedures. A fatigue strength value was determined using a method developed by Hamilton Sundstrand. The period of testing spanned January through November 1999.					
15. SUBJECT TERMS Mechanical Properties Aluminum Alloy 7076-T6 54H60 Propeller Blades					
16. SECURITY CLASSIFICATION OF:			17. LIMITATION OF ABSTRACT UL	18. NUMBER OF PAGES 28	19a. NAME OF RESPONSIBLE PERSON Kenneth George
a. REPORT Unclassified	b. ABSTRACT Unclassified	c. THIS PAGE Unclassified			19b. TELEPHONE NUMBER (include area code) 301-342-8022

Standard Form 298 (Rev. 8-98)
Prescribed by ANSI Std. Z39-18

SUMMARY

This report documents a collaborative material characterization study of 7076-T6 forged aluminum performed by the NAVAIRSYSCOM Materials Division and Hamilton Sundstrand, sponsored and coordinated by the NAVAIRSYSCOM Engineering Specialties Division. The purpose was to determine the mechanical properties of the alloy to support the development of a fatigue allowables curve used for life assessment of 54H60 propeller blades. Specimens were fabricated from unused propeller forgings and tested at room temperature in ambient laboratory conditions using servo-hydraulic mechanical testing equipment. Tensile properties, fatigue crack growth rates, and stress life behavior were characterized using standard ASTM test procedures. A fatigue strength value was determined using a method developed by Hamilton Sundstrand. The period of testing spanned January through November 1999.

CONTENTS

	<u>Page No.</u>
Summary	ii
Acknowledgments	iv
Introduction	1
Background	1
Methods	1
Specimen Preparation	1
Tensile Tests	1
Fatigue Crack Growth Testing	2
Stress Life Testing	2
Fatigue Strength	3
Discussion	3
Microscopy	3
Tensile Properties	4
Fatigue Crack Growth	4
Stress Life	4
Cyclic Fatigue Strength	5
Conclusions	7
Recommendations	7
References	9
Appendices	
A. Figures	11
B. Tables	17
Distribution	21

ACKNOWLEDGEMENTS

The authors would like to thank Ms. Veena Agarwala and Mr. Jack Dennison for their assistance in report review and metallographic sample preparation, and Mr. Henry Sanders for assistance in conducting mechanical testing.

INTRODUCTION

BACKGROUND

This study was undertaken to provide mechanical property data of forged 7076-T6 aluminum for the compilation of a fatigue allowables curve in development by the NAVAIRSYSCOM Engineering Specialties Division and Hamilton Sundstrand (HS). Although HS had derived much of the data for this curve from full-scale testing of 54H60 helicopter blades, additional fatigue testing was required at the specimen level to determine the cyclic fatigue strength of 30 million cycles. All specimens were machined and tested in accordance with ASTM standards E 8, E 466, and E 647. Specimens were machined from three virgin forged 54H60 blade shank sections. The fatigue strength was determined by a staircase method developed by HS. Supplemental testing included determination of Young's modulus, 0.2% yield strength, tensile strength, elongation, and reduction of area. Also, the fatigue crack growth (FCG) behavior was characterized as crack growth increment per cycle (da/dN) versus change in stress intensity (ΔK) from threshold (ΔK_{th}) through critical crack growth. All tests were performed in ambient laboratory air using MTS digitally controlled, servo-hydraulic universal test frames. The integration of the full-scale and laboratory tests into the fatigue allowables curve is beyond the scope of this report.

METHODS

SPECIMEN PREPARATION

The 54H60 blade shank section geometry and specimen orientation are shown in figure A-1. HS cut the forgings into 3/4-in. thick slabs parallel to the shank axis and shipped them to the NAWCAD Patuxent River, Maryland, Materials Division. Upon receipt, the direction of grain flow was established by evaluating metallographic samples taken from the locations numbered 3-10 in figure A-1. The material was then marked to indicate grain orientation and sent to NAWCAD Lakehurst for machining. Ten compact tension (CT) fatigue crack growth specimens were machined in the L-C orientation; approximately 70 S-N fatigue specimens and 6 tensile specimens were machined in the L-orientation. Specimen type and identification was randomized among the three forgings in an attempt to average the material properties.

The CT specimens were electrodischarge machined in an integral knife edge configuration with thickness and width dimensions of $B=0.375$ in. and $W=1.5$ in., respectively. Surfaces were polished to a mirror finish to facilitate visual observations of crack length. Tensile specimens were machined round with a 1 in. gage length and a 0.25 in. reduced diameter. S-N specimens were machined round with a continuous radius and 0.25 in. reduced diameter. Both were lathe turned and then polished by successive steps finishing with 800-grit emery cloth.

TENSILE TESTS

Tensile testing was conducted at a crosshead speed of 0.05 in./min, a load cell range of 5,000 lb, and an extensometer range of 0.05 in. Hydraulic gripping fixtures were aligned to assure a maximum bending strain of less than $10 \mu\epsilon$ using an alignment fixture, strain-gauged specimens, and specialized software. Modulus calculations were made by linear regression analysis using

data taken while loading the tensile specimens between 10 and 80% of the elastic range. They were then pulled to failure, and the 0.2% yield strength and tensile strength was determined. Elongation and reduction in area measurements were made post-test by fitting the broken ends together.

FATIGUE CRACK GROWTH TESTING

FCG testing at stress ratios (R) of R=0.1 and R=0.4 was performed at a test rate of 10 Hz with respective load cell and clip gage ranges of 1,000 lb and 0.02 in. Crack length was calculated in real time using specimen compliance and an FTA automated crack growth system. Accuracy and even crack growth was assured by periodical visual observations. Precracking was initiated at 700 lb at R=0.1 with 20% load shed intervals until a target FCG rate of 2×10^{-7} in./cycle was achieved with sufficient precrack length to satisfy linear-elastic requirements. The final length of precracking was conducted at the R of interest using constant K control to eliminate transient effects.

The FCG behavior was characterized for each specimen from ΔK_{th} to a crack growth rate of approximately 10^{-5} in./cycle by combining data obtained from a two-step process of decreasing K and constant load. First, the lower region of the curve was obtained by starting at the final precrack load and applying a K-gradient of $C=-2 \text{ in.}^{-1}$. Testing was terminated when the crack growth rate approached 10^{-9} in./cycle. Then the upper portion of the da/dN curve was determined by resuming at a load corresponding to an FCG rate just below 10^{-7} in./cycle and allowing the crack to grow under constant load control. Data collected from both steps were superimposed to construct a single plot of the entire range. Quantitative data extracted from these curves included ΔK_{th} values as well as the coefficients and exponents of the expression $da/dN = C\Delta K^n$ for crack propagation rates between the range of 2×10^{-7} to 10^{-5} in./cycle.

STRESS LIFE TESTING

Standard stress life testing was performed at R=0.1 and R=0.4 at 30 Hz using hydraulic collet grips aligned in the same manner as the tensile tests with a load cell range of 5 Kip. The objective of stress life testing was twofold. First, the alloy was to be characterized on an S-N diagram. Then, the data were to be curve fit to extrapolate a starting point for a subsequent cyclic fatigue strength determination. The bounds of the S-N curve were defined as an upper stress level equal to 95% the tensile yield stress and a lower stress level corresponding to an average fatigue life of 10^6 cycles. The lower value was found empirically using published Goodman data (reference 1) as a guideline. A 20-specimen test matrix was executed between these two endpoints with five data point sets at four discrete stress levels. The stress levels used were 47, 51, 57, and 63 ksi for R=0.1 and 58, 60, 62, and 64 ksi for R=0.4.

FATIGUE STRENGTH

The HS procedure (reference 2) for determining the cyclic fatigue strength was performed as follows: an initial estimate of the fatigue strength, X , was made by curve fitting the S-N data described earlier to extrapolate the stress corresponding to the fatigue strength of interest. For this case, it was the stress corresponding to 30×10^6 cycles. Using this as a 100% baseline value, six specimens were fatigued in staircase fashion by starting at 80% of X and cycled until failure or run out (30×10^6 cycles) occurred. Then the stress was increased by a percentage increment, and the test was repeated on the survivors. Through discussions with the sponsor, the stress increments in terms of percents of X were set as 80, 90, 100, 105, and 110%.

Failure data for specific R values were then plotted on a semi-log chart. A straight line was fitted through the left most failure (lowest number of cycles irrespective of stress level) and its previous run-out data point. Using the slope of this line, five additional lines were drawn through the other failure data intersecting the 30×10^6 vertical marker line. At this intersection, the corresponding stress was recorded and the mean calculated. This value was then defined as the fatigue strength.

Due to the time associated with the staircase portion of testing, the sponsor coordinated a collaborative effort between HS and the Materials Division. HS was to conduct 8 of the 12 staircase tests; however, only 5 tests were completed within the study's time frame. HS used specimens provided by the Materials Division and modified them for use in threaded grips. Survivor specimens tested in hydraulic grips tended to fail in the grip section after two to three consecutive tests. This was corrected by repolishing the grip section each time run out was achieved and by using the lowest possible grip pressure.

DISCUSSION

MICROSCOPY

Metallographic samples elucidated two basic grain morphologies with a transition occurring at Line A of figure A-1. Grain flow above this line deviated outward in the radial direction and became equiaxed as shown in figure A-2. This micrograph corresponds to the L-R direction, location No. 5 of figure A-1, and illustrates the decreasing effect of the forging operation on microstructure in this region. In comparison, all micrographs taken from samples below Line A consistently demonstrated similar deformation morphology in terms of grain size, aspect ratio, and flow direction as depicted in figure A-3, which corresponds to the L-R direction, location No. 3. This suggested uniform deformation and work hardening throughout the lower portion of the forging with no evidence of appreciable morphology variance with respect to radial or longitudinal position. As a result of this analysis, only material below Line A was used for specimen fabrication.

TENSILE PROPERTIES

Tensile data are summarized in table B-1. The relatively small standard deviations of tensile properties throughout the forging indicated that each of the forgings was processed similarly with respect to heat treat and work hardening. This is consistent with the results of the metallographic analysis. Selected data (reference 3) of similar aluminum alloys are shown for comparison purposes.

FATIGUE CRACK GROWTH

A representative plot of the overall FCG behavior for both $R=0.1$ and $R=0.4$ is shown in figure A-4. The higher $R=0.4$ data are shifted to the left, corresponding to an overall decrease in fatigue crack growth resistance with increasing R . This shift can be quantified by observing the data in table B-2. In terms of the shift from $R=0.1$ to $R=0.4$, we see a 28% decrease in ΔK_{th} . For the region of crack growth between the rates of 2×10^{-7} and 10^{-5} in./cycle, the shift is characterized by the coefficient of the corresponding rate expression $da/dN = C\Delta K^n$. This effect can be visually observed in figure A-4. For example, the crack growth rate at a constant $\Delta K = 5 \text{ ksi}\sqrt{\text{in.}}$ is one order of magnitude greater for $R=0.4$ compared to $R=0.1$. For aluminum alloys in laboratory air at a frequency of 10 Hz, this phenomenon is most likely a result of the increased mean load and decreased amount of crack closure at the higher R .

A curious feature of these curves is the behavior of the crack growth rate near the 10^{-5} in./cycle regime. The curves tend to bend to the right signifying a marked decrease in growth rate. At this point, the test validity was verified with respect to linear elastic test requirements of remaining ligament and plastic zone size. In addition, the crack length was found to be within acceptable bounds of the compliance measurement technique. The sponsor provided unpublished data of this alloy collected by the NASA Johnson Space Center, which also exhibited this tendency. Therefore, it was concluded that this is an inherent property of the material worthy of further investigation.

STRESS LIFE

Figures A-5 and A-6 are compilations of the stress life data acquired for $R=0.1$ and $R=0.4$. Typical face-centered cubic fatigue behavior (reference 4) is noticed for the $R=0.1$ data with the S-N curve bipartitioning into two regions intersecting at approximately 10^5 cycles. However, the $R=0.4$ data do not demonstrate such an identifiable partition. It is unclear if this is a result of the large amount of scatter relative to the data of $R=0.1$, the higher mean load, or some combination. In any case, the $R=0.1$ curve is shifted down and to the left in comparison to $R=0.4$ demonstrating a decrease in fatigue crack initiation resistance with decreasing R and increasing stress amplitude.

CYCLIC FATIGUE STRENGTH

The results of the stress life testing were used to estimate a starting point for the cyclic fatigue strength determination by curve fitting the data and extrapolating the stress, X , corresponding to a life of 30×10^6 cycles. The applied power law curve fit expressions, graphical representations, and corresponding R^2 values are shown on the S-N curves in figures A-5 and A-6.

The two lower most data sets of the $R=0.1$ data were assumed to approximate a straight line fit with no endurance limit (reference 4). These data were fit between 47 and 51 ksi yielding an $X = 43$ ksi when rounded to the nearest whole number. Inspection of figure A-5 suggests that this was a reasonable estimate. For the case of $R=0.4$, a bipartition was not discernable, so all the data between 60 and 64 ksi were used yielding $X = 59$ ksi. Visual observations of figure A-6 suggest that this estimate was high, as the line shown is too shallow to intersect the 60 ksi data set. Table B-3 was then constructed to identify the stress levels to be used for staircase testing by taking the values of X found above as 100% and calculating the other required percentages thereof. HS opted to round these values to the nearest ksi during staircase testing.

Table B-4 contains the staircase test matrix showing the division of work and test results. Specimen No. 38 was tested first at stress levels of 80, 90, and 100% X achieving run out at each increment and failing at the 45.2 ksi (105%) level. Therefore, it was mutually decided that in the interest of time, all remaining $R=0.1$ tests would be started at the 90% level. During testing, specimen No. 71 was inadvertently started at the 100% level and failed at 1,134,112 cycles. However, this was taken as a valid data point because it was reasonable to assume that the specimen would have attained run out at 90% due to the relatively large amount of cycles attained at the 100% level. Both $R=0.4$ specimens tested by the Materials Division failed at the 90% level while those tested by HS tests failed at 100%. Specimen Nos. 35, 48, and 53 were not completed, resulting in only five usable data points at $R=0.1$ and four at $R=0.4$.

The data from table B-4 were used as source data to create the construction plots shown in figures A-7 and A-8. Specimen No. 71 was the left most failure point of the $R=0.1$ data of figure A-7. A line through this point and its previous run out established the slope of the line to be applied to the remaining data. The run-out value of No. 71, extrapolated stresses, and final fatigue strengths are shown in table B-5. Similar methodology was used to obtain the data for $R=0.4$.

Calculating the mean value of the stresses and rounding to the nearest ksi give fatigue strengths of 42 ksi for $R=0.1$ and 52 ksi for $R=0.4$. Comparing these data to the original estimates shows that the $R=0.1$ estimate was reasonably close with a difference of 1 ksi. The $R=0.4$ data, however, resulted in a larger difference of 7 ksi. In addition to the cyclic fatigue strength, the standard deviation was calculated to find the strength minus three-sigma value. The final cyclic fatigue strength and the fatigue strength minus three-sigma values are included in table B-5 and depicted graphically in figures A-5 and A-6. This provides some indications as to the accuracy and limitations of the method.

Since the entire test matrix was not completed, a complete evaluation of the method and statement of accuracy of the results is not possible. However, some qualitative information can be assessed. For example, inspection of figures A-5 and A-6 shows that agreement of the estimate and the final result is most likely a function of the curve fitting parameter. An R^2 value of 0.8199 for the $R=0.1$ data yielded a closer agreement between the initial estimate and final result than that of the $R=0.4$ data, which had a lower R^2 value of 0.3588. Therefore, to improve the estimate, either additional specimens should be run or an alternative curve fit methodology must be found.

There is some indication, however, that the staircase method may not require absolute accuracy of the estimate to provide a reasonable result. Consider the data of figure A-6. Although the power law expression used provided an estimate that was clearly high, the resulting cyclic fatigue strength value is closer to what one would intuitively expect. This suggests that the method has a certain degree of inherent robustness. Assuming this thinking is correct, one could argue a priori that the stress life behavior shown in figure A-6 does not exhibit a bipartition of data. This fact is masked by the scatter of the data, but may be elucidated by the result of the staircase tests. Clearly, more testing is required to confirm these assumptions.

CONCLUSIONS

The forging and heat treating processes employed in the manufacture of the 7076-T6 alloy used for this study produced material of consistent grain structure and material properties. Tensile strength and elongation properties of the alloy tested are superior to that of 7076-T61 property data found in the literature.

The results of stress life testing demonstrated a downward shift in the fatigue data with decreasing R, indicating a decrease in fatigue initiation resistance with decreasing R. In contrast, plots of FCG behavior data demonstrated a shift to the left with increasing R, corresponding to a decrease in fatigue crack growth resistance with increasing R. This shift was quantified in the lower region of the da/dN curve by a 28% reduction in ΔK_{th} as well as a large change in the coefficient of the rate expression. FCG curves of this alloy exhibit a decrease in crack growth rate near da/dN values of 10^{-5} in./cycle.

R=0.1 stress life testing produced a classic FCC-type S-N curve with well-grouped data and a clear bipartition. The R=0.4 data, however, were not as well-behaved and characterized by orders of magnitude of scatter at each stress level. Linear curve fitting to attain an estimate of cyclic fatigue strength was better suited to the R=0.1 data as opposed to the R=0.4 data as evidenced by visual inspection of the resulting lines and their associated R^2 values.

Execution of the HS method of staircase testing and analysis yielded cyclic fatigue strengths of 42 ksi for R=0.1 and 52 ksi for R=0.4. The R=0.1 result was within 1 ksi of the original estimate while the result for the R=0.4 differed by 7 ksi. Accuracy of the estimation using a power law fit requires a certain degree of correlation that may be improved by additional testing and/or alternative curve fit procedure. Also, the staircase method appears to have some inherent robustness that allows for some error in the initial estimate of the starting point.

RECOMMENDATIONS

Validation of the method within this report, development of other stress life methodologies, or future long-term materials characterizations could be completed using newly available high frequency test machines in a relatively short amount of time.

The minimum number specimens required to produce the baseline S-N curves for a cyclic fatigue strength determination is a function of the correlation of the results. Guidance should be established as to what is an acceptable level of correlation when curve fitting these results, which should drive the number of specimens needed.

In terms of fundamental material properties, an investigation could be made as to why the material exhibits a reduction in FCG rate in the region of 10^{-5} in./cycle. The study should concentrate on this crack growth regime and possibly use larger sized specimens to eliminate the chance of any size influence.

THIS PAGE INTENTIONALLY LEFT BLANK

REFERENCES

1. Fatigue Data Book, American Society of Metals, Metals Park, OH, 1995, p 102.
2. H. J. Grover, S. A. Gordon, and L. R. Jackson, The Fatigue of Metals and Structures, Battelle Memorial Institute, Prepared for Bureau of Naval Weapons, Dept. of the Navy, NAVWEPS 00-25-534, 1954, Revised 1960.
3. ASM Handbook, Volume 2, Properties and Selection: Nonferrous Alloys and Special Purpose Materials, American Society for Metals, Metals Park, OH, 1990, pp 116-118.
4. Planning and Evaluation of Fatigue Tests, ASM Handbook, Volume 19, Fatigue and Fracture, American Society for Metals, Metals Park, OH, 1996, pp 303-313.

THIS PAGE INTENTIONALLY LEFT BLANK

**APPENDIX A
FIGURES**

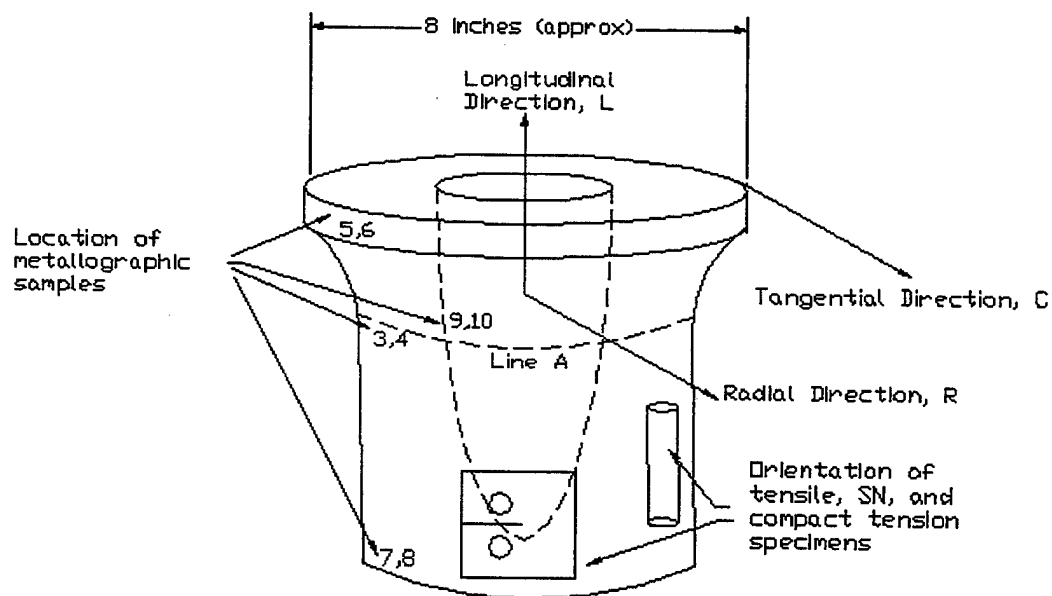


Figure A-1: Schematic of 7076 Aluminum Propeller Forging Original Geometry Before Sectioning, Specimen Orientation and Approximate Location, and Location of Metallographic Samples

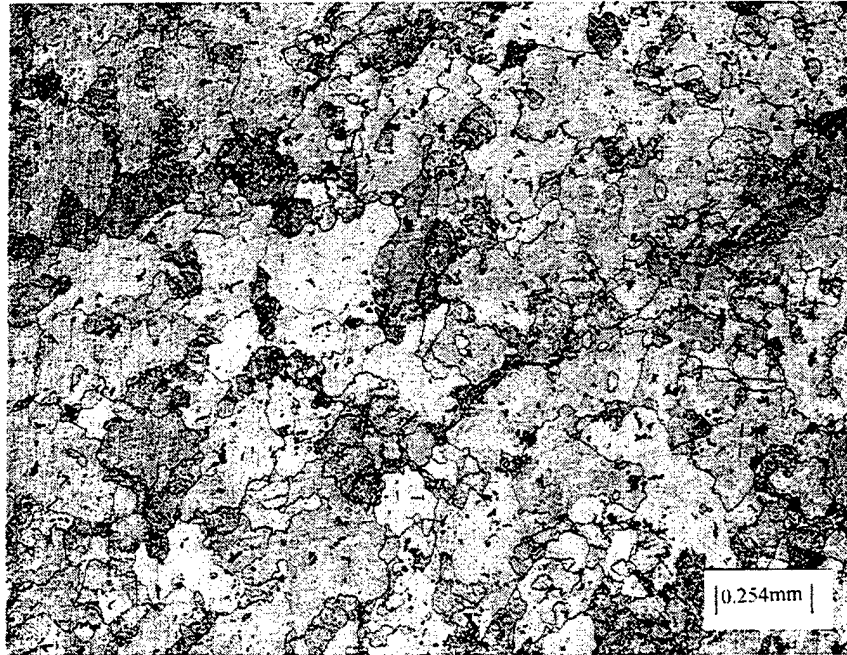


Figure A-2: Grain Morphology of Discarded Material Showing Equiaxed Morphology With Little Influence of the Forging Operation



Figure A-3: Typical Alloy Microstructure of Specimen Material Showing Consistent Grain Flow in the Longitudinal Direction With Respect to the Forging Operation

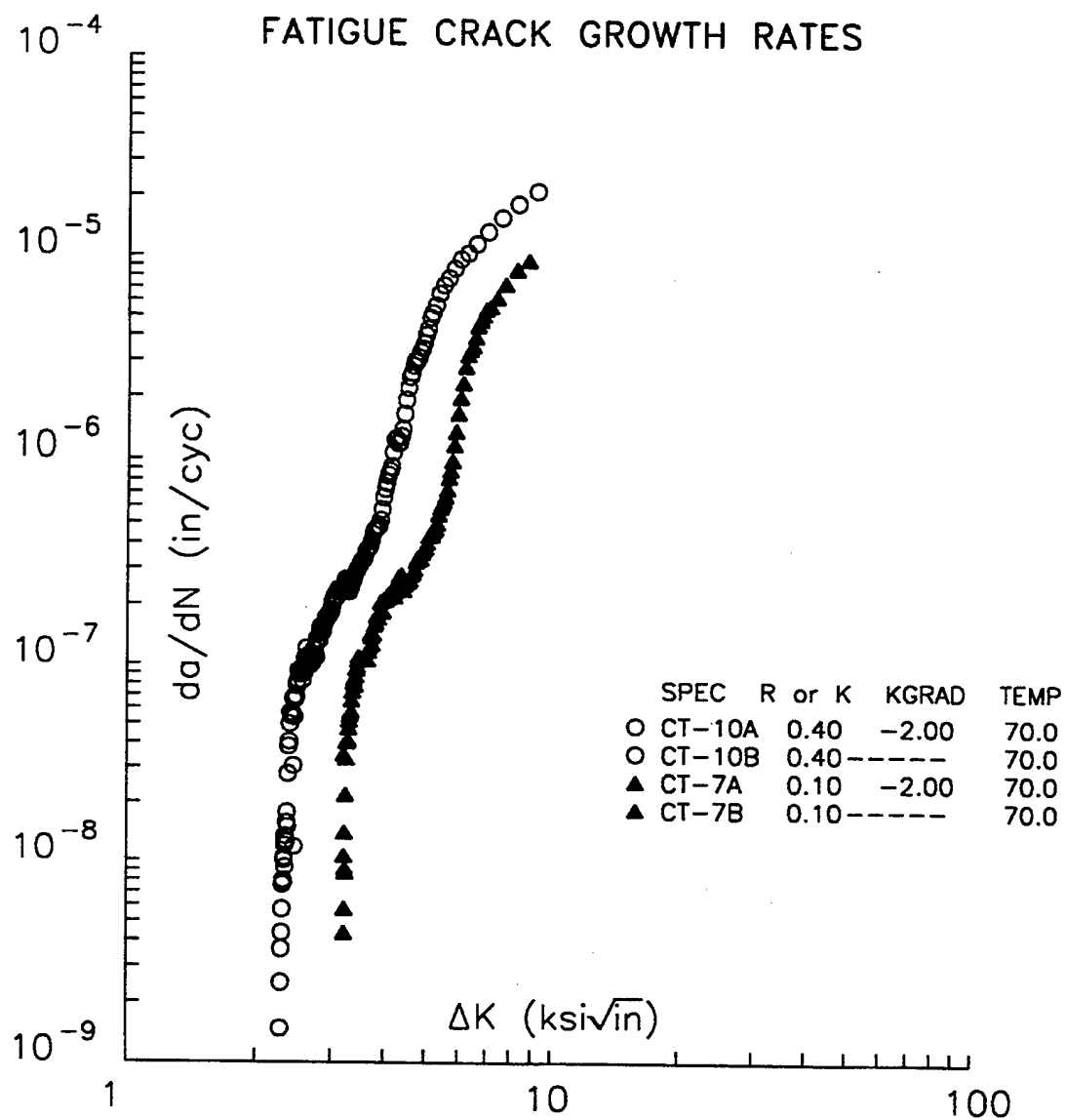


Figure A-4: Plot Depicting Typical FCG Behavior at R=0.1 and R=0.4

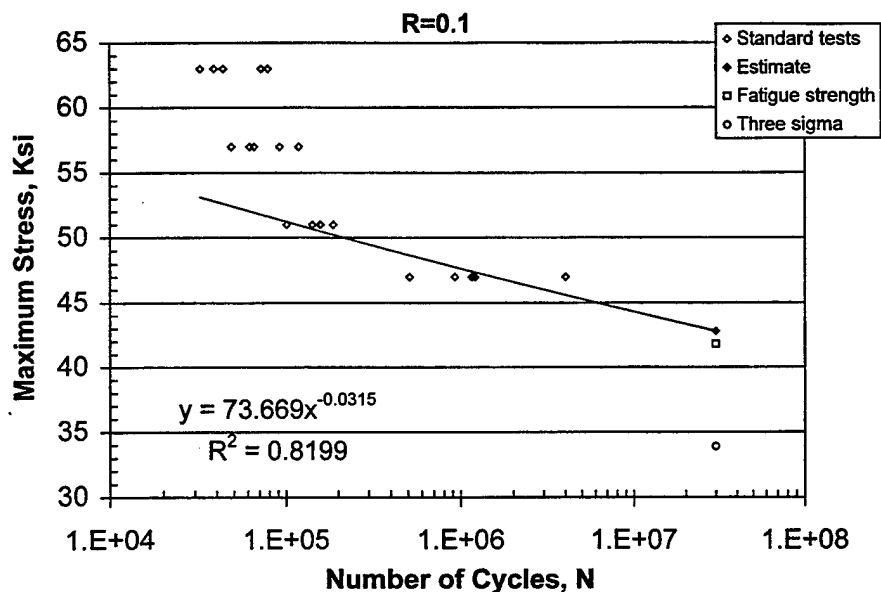


Figure A-5: Results of Stress Life Testing at R=0.1 Including Standard Tests, Curve Fit and Initial Fatigue Strength Estimate, Fatigue Strength, and Minus Three Sigma Fatigue Strength

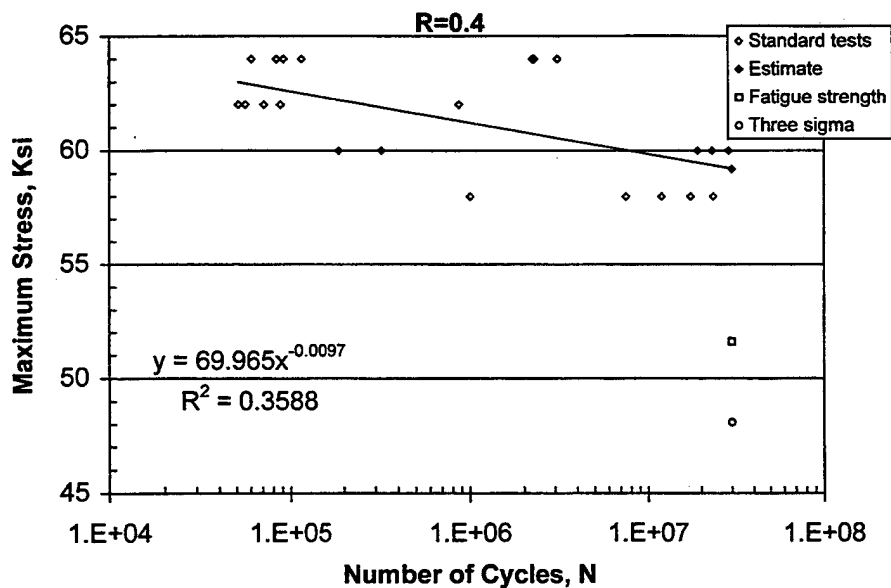


Figure A-6: Results of Stress Life Testing at R=0.4 Including Standard Tests, Curve Fit and Initial Fatigue Strength Estimate, Fatigue Strength, and Minus Three Sigma Fatigue Strength

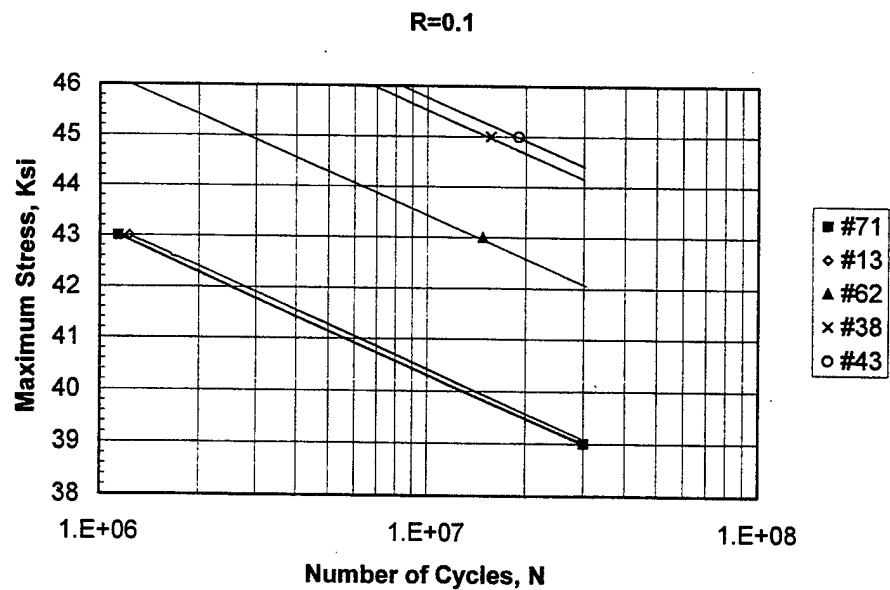


Figure A-7: R=0.1 Fatigue Strength Construction Plot

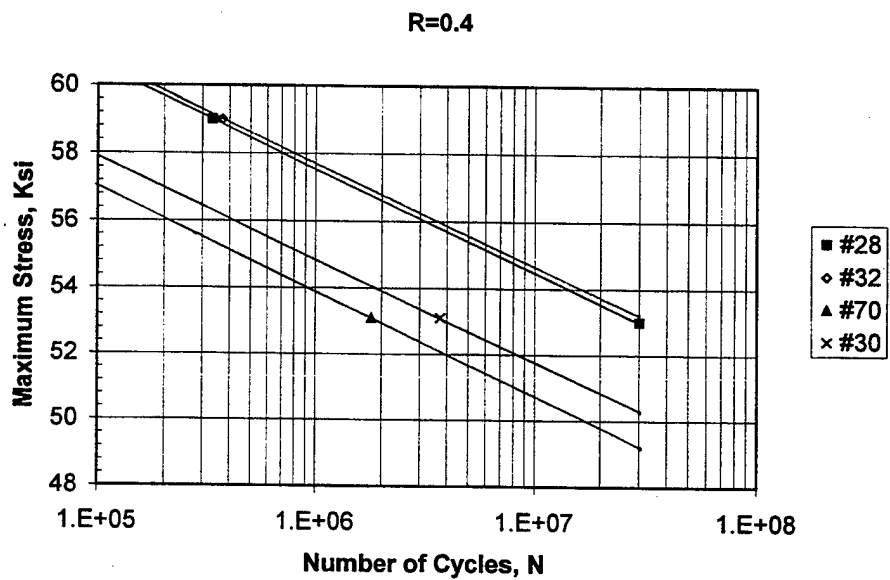


Figure A-8: R=0.4 Fatigue Strength Construction Plot

**APPENDIX B
TABLES**

Table B-1: Summary of Tensile Data

Specimen	Initial Diameter (in.)	0.2% yield (ksi)	Tensile Strength (ksi)	Elongation (%)	Reduction in Area (%)	Modulus (msi)
T1-E	0.2510	64.8	73.6	17.5	17.7	10.0
T2-I	0.2490	66.5	74.8	20.0	18.6	9.9
T3-I	0.2485	67.0	75.0	17.0	18.6	10.1
T5-S	0.2500	66.7	74.6	19.0	18.9	10.0
T7-S	0.2505	66.8	74.8	17.1	19.3	10.0
T8-S	0.2495	67.4	75.0	16.0	17.6	10.3
7076-T6 ⁽¹⁾	--	60	70	14 (2 in.)	--	9.7
7075-T6 ⁽¹⁾	--	73	83	11	--	10.3
Average:		66.5	74.6	17.8	18.5	10.1
Standard Deviation:		0.9	0.5	1.5	0.7	0.1

NOTE: (1) Presented for comparison purposes only (reference 3).

Table B-2: Fatigue Crack Growth Data Showing FCG Threshold Values and Crack Growth Coefficients and Exponents for $da/dN = C\Delta K^n$ Between Crack Growth Rates of 2×10^{-7} and 10^{-5} in./Cycle

Specimen	R-Ratio	ΔK_{th} ksi $\sqrt{in.}$	C in. ^{1/2} /(cyc*ksi)	n
CT-3	0.1	3.12	2.018E-11	6.360
CT-4	0.1	2.92	3.828E-11	6.022
CT-6	0.1	2.73	9.165E-11	5.640
CT-7	0.1	3.22	3.210E-11	6.050
Average:		3.00	4.556E-11	6.018
Standard Deviation:		0.22	3.164E-11	0.295
CT-2	0.4	2.24	7.991E-11	6.717
CT-5	0.4	1.98	2.164E-10	6.079
CT-8	0.4	2.12	3.735E-10	5.521
CT-10	0.4	2.29	1.501E-10	6.269
Average:		2.16	2.050E-10	6.147
Standard Deviation:		0.15	1.254E-10	0.495

Table B-3: Calculated Values for Staircase Tests

R=0.1	R=0.4
X = 43 ksi	X = 59 ksi
0.8 (43) = 34.4	0.8 (59) = 47.2
0.9 (43) = 38.7	0.9 (59) = 53.1
1.0 (43) = 43.0	1.0 (59) = 59.0
1.05 (43) = 45.2	1.05 (59) = 62.0
1.1 (43) = 47.3	1.1 (59) = 65.9

Table B-4: Results of Staircase Testing

Specimen No.	R	Maximum Stress (ksi)	No. of Cycles
NAWCAD Patuxent River Tests			
38	0.1	34.4	Run Out
38	0.1	38.7	Run Out
38	0.1	43.0	Run Out
38	0.1	45.2	15,620,588
71	0.1	43.0	1134112
30	0.4	47.2	Run Out
30	0.4	53.1	3,717,058
70	0.4	47.2	Run Out
70	0.4	53.1	1,791,873
Hamilton Sundstrand Tests			
13	0.1	39	Run Out
13	0.1	43	1,227,000
43	0.1	39	Run Out
43	0.1	43	Run Out
43	0.1	45	19,000,000
62	0.1	39	Run Out
62	0.1	43	14,814,000
35	0.1	39	Run Out
35	0.1	43	Run Out
35	0.1	45	Run Out
35	0.1	47	Not Tested
28	0.4	53	Run Out
28	0.4	59	332,965
32	0.4	53	Run Out
32	0.4	59	370,630
48	0.4	53	Run Out
48	0.4	59	Not Tested
53	0.4	53	Not Tested

Table B-5: Extrapolated Stress Values and Calculated Mean Corresponding to a 30×10^6 Cycle Fatigue Strength

Specimen No.	Extrapolated Stress, ksi at 30×10^6 Cycles
R=0.1	
71 (left most failure)	39 (run out)
13	39.2
62	42.2
38	44.2
43	44.5
35	Not tested
	Mean = 41.8
	$\sigma = 2.6$
	Mean- $3\sigma = 33.9$
R=0.4	
28 (left most failure)	53
32	53.2
70	50.6
30	49.8
48	Not tested
53	Not tested
	Mean = 51.6
	$\sigma = 1.7$
	Mean- $3\sigma = 48.1$

DISTRIBUTION:

NAVAIRSYSCOM (AIR-4.3.4.2)	(10)
NAVAIRSYSCOM (AIR-4.4.7.2)	(5)
NAVAIRWARCENACDIV Patuxent River, MD (Technical Publishing Team)	(1)
DTIC	(1)